Available online at www.sciencedirect.com
ScienceDirect
Journal of Power Sources 173 (2007) 592–598
JOURNAL OF POWER SOURCES
www.elsevier.com/locate/jpowsour

Magnesium batteries: Towards a first use of graphite fluorides

Jérôme Giraudet [a,*], Daniel Claves [a], Katia Guérin [a], Marc Dubois [a], Axel Houdayer [a], Francis Masin [b], André Hamwi [a]

[a] *Laboratoire des Matériaux Inorganiques, UMR CNRS 6002, Université Blaise Pascal, 24 av. des Landais, 63177 Aubière Cedex, France*

[b] *Matière Condensée et Résonance Magnétique, Université Libre de Bruxelles (U.L.B.), CP 223, Boulevard du Triomphe, B-1050 Bruxelles, Belgium*

Received 27 October 2006; received in revised form 3 April 2007; accepted 29 April 2007
Available online 5 May 2007

Abstract

Graphite fluorides obtained by fluorination of graphite at room temperature and after a subsequent re-fluorination treatment were characterised by X-ray diffraction and ^{19}F MAS NMR. Their electrochemical performances as cathode materials in magnesium batteries have been investigated. Four different electrolytes (0.5 or 1 M $Mg(ClO_4)_2$ in ACN, DMSO, PC and THF) were used for these tests. The specific energy and power densities were estimated for all media. A comparison of the performances between lithium and magnesium batteries was realised. The effect, on the electrochemical performances, of a re-fluorination treatment at 250 °C was also studied.

Keywords: Graphite fluoride; Magnesium batteries; Electrochemical properties

1. Introduction

Progress in portable electronic devices requires more and more efficient batteries. Ion-transfer batteries are well adapted for such applications. Up to date, most of the research performed in this field concerns lithium intercalation batteries [1,2]. In answer to the two important problems regarding the cost of such batteries and their environmental impact, magnesium, because of its high natural abundance and lesser harm in comparison with lithium, seems to be a promising alternative for negative electrodes. However, the standard potential of the aqueous Mg^{2+}/Mg redox couple is 0.66 V higher than the one of Li^+/Li (Fig. 1), which prefigures a lower discharge potential for magnesium batteries, in addition to a lower energy density due to a smaller specific capacity-to-weight ratio for magnesium [3]. A magnesium battery is then a compromise between a high performance system and a lower cost one. Magnesium intercalation has been less studied than lithium intercalation. The following and non-exhaustive list gives some examples of materials allowing accommodation of magnesium under ionic form: transition metals oxides (V_2O_5 [4,5], MoO_3 [6], $Mn_yCo_zO_4$ [7], ...), sulphides (TiS_2 [8], NbS_3 [9], $Mg_xMo_3S_4$ [10], ...), and borides (MoB_2 [8], TiB_2 [8], ...).

Graphite fluorides have already been extensively studied as cathode materials in lithium [11–17] or aluminium batteries [18]. Thus, covalent graphite fluorides yield a discharge capacity of about 900 Ah kg^{-1} associated to a discharge potential close to 2.1 V versus Li^+/Li [11–13]. For aluminium batteries, the discharge potential and capacity are close to 1 V versus Al^{3+}/Al and 500 Ah kg^{-1} [18], respectively. Interestingly, graphite fluorides prepared according to the method developed earlier by Hamwi et al. [19,20], i.e. fluorination at room temperature using a catalytic gaseous mixture of F_2, HF, MF_n, where MF_n is IF_5, BF_3, WF_6, ... strongly increases the discharge potential up to 3 V versus Li^+/Li, though a decrease of the capacity is observed concomitantly [14].

Hence, graphite fluorides in association with magnesium may appear as interesting cell-components. In our study, we have investigated, for the first time, the behaviour of graphite fluoride prepared by fluorination of graphite at room temperature, toward magnesium accommodation. The influence of both the

* Corresponding author. Present address: Matière Condensée et Résonance Magnétique, Université Libre de Bruxelles (U.L.B.), Belgium.
Tel.: +32 2 650 5023; fax: +32 2 650 5675.
E-mail address: jerome.giraudet@ulb.ac.be (J. Giraudet).

0378-7753/$ – see front matter © 2007 Elsevier B.V. All rights reserved.
doi:10.1016/j.jpowsour.2007.04.067

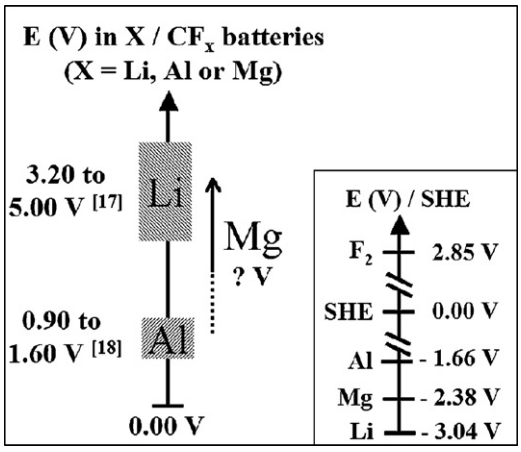

Fig. 1. Electrochemical potentials for X/CF_x batteries (X = Al, Li or Mg). Inset shows the standard potentials (vs. SHE electrode) for Li, Mg, Al and F_2.

electrolyte medium and the thermal post-treatment under fluorine, on the electrochemical performances, was also studied. A comparison with the electrochemical properties observed upon lithium insertion is given.

2. Experimental

2.1. Sample preparation

The starting material was a natural graphite powder from Madagascar with average grain size of about 4 μm. A sample, denoted $CF(IF_5)$, was first prepared according to a room temperature synthesis route using an iodine fluoride (IF_5), hydrogen fluoride (HF) and fluorine (F_2) gaseous mixture, as described in Ref. [19]. Re-fluorination of the former $CF(IF_5)$ product was carried out under pure F_2 gas at 250 °C, as described in Ref. [21,22], resulting in sample denoted CF(250). According to weight uptake, the following apparent chemical formulae were obtained: $CF_{1.03}$ and $CF_{0.88}$ for $CF(IF_5)$ and CF(250), respectively. As previously shown [21,22] for the raw fluorination product or for re-fluorination temperatures up to 250 °C, part of mass uptake must be assigned to some residual iodine and not to fluorine atoms bonded to carbon. Hence, the true chemical formulae obtained by chemical analysis were $CF_{0.73}(IF_5)_{0.02}(HF)_{0.06}$ for $CF(IF_5)$ and $CF_{0.76}(IF_5)_{0.01}$ for CF(250).

2.2. Physical characterization

^{19}F Magic Angle Spinning (MAS) Nuclear Magnetic Resonance (NMR) experiments were performed on a Bruker MSL 300 spectrometer (working frequency of 282.2 MHz) with a 4 mm Cross Polarization/Magic Angle Spinning probe from Bruker. The spinning speed employed was between 12 and 14 kHz. A simple sequence (τ-acquisition) was used with a $\pi/2$ pulse length of 4 μs. All chemical shifts were referenced with respect to $CFCl_3$.

X-ray diffraction (XRD) powder patterns were obtained using a Siemens D501 diffractometer working with the Cu Kα radiation.

2.3. Electrochemical study

Typical electrodes were composed of graphite fluoride (about 70 wt%), graphite powder (10%) and carbon black (10%) to ensure electronic conductivity, and polyvinylidene difluoride (PVDF, 10%) as binder. After stirring in propylene carbonate (PC), this mixture was spread thinly onto a stainless steel current collector disc (diameter of 10 mm) by evaporation of PC; then it was heated at ≈ 100 °C under vacuum to remove traces of water and solvent. The mass of active carbon are close to 1 mg for all experiments. A two electrodes system was used (Swagelok cell type), where magnesium was both reference and counter electrode. A PVDF microporous film, wet with electrolyte, was sandwiched between the composite electrode and a magnesium metal foil (0.25 mm^2). In order to eliminate the surface oxide film, the Mg was previously washed with diluted HCl solution. Several electrolytes were tested: 1 M $Mg(ClO_4)_2$/ACN (acetonitrile), 0.5 M $Mg(ClO_4)_2$/DMSO (dimethylsulfoxide), 1 M $Mg(ClO_4)_2$/PC (propylene carbonate) and 1 M $Mg(ClO_4)_2$/THF (tetrahydrofuran) (+3.33 M H_2O/THF). The electrolyte solvents were doubly distilled prior to use. The perchlorate salt and the magnesium foil were commercial products, Aldrich and Alfa Aesar, respectively. The cells were assembled under argon in a glove box. Galvanostatic discharges were recorded with a VMP2-Z from Biologic, at room temperature and under a 10 A kg^{-1} current density.

3. Results and discussion

3.1. Characterization of the graphite fluorides

Preliminary characterisation of all the samples studied was necessary to better understand the behaviour of each material and the electrochemical mechanisms. Fig. 2a displays the X-ray diffraction patterns of the two graphite fluoride samples. Four reflections are observed. The first one, at about 14° (d = 0.631 nm), is typical of the (0 0 1) reflection of a first stage fluorine graphite intercalation compound. The second, near 21° (interlayer distance d = 0.423 nm), corresponds to a residual first stage graphite intercalation compound with IF_z ($z \approx 5$; presence of IF_5, IF_6^- and IF_7 with IF_5 as main species). The remaining features, at 41–42° (d = 0.220 nm) and 78° (d = 0.123 nm), represent the (1 0 0) and (1 1 0) reflections issuing from graphite planes, respectively. Accordingly, the repeat distance along the c axis in the $CF(IF_5)$ sample is 0.598 nm and the C–C bond length is 0.143 nm, which is typical of sp^2 hybrydizated carbon atoms. Upon re-fluorination at 250 °C, the only structural change is an expansion of the interlayer spacing to 0.638 nm for CF(250). This fact is explained by a more important F/C ratio in the latter sample.

^{19}F MAS NMR (Fig. 2b), provides further information about the iodine species content, mainly IF_5 ($\delta_{^{19}F} \approx 2$ and 50 ppm) and IF_6^- ($\delta_{^{19}F} \approx 11$ ppm), whose variations are not easily revealed by the X-ray diffraction data. The position of the observed NMR lines also reflects the nature of the C–F bond character.

Inset in Fig. 2b shows the typical lines (all line intensities normalised to the same value) of the IF_z catalysts over the

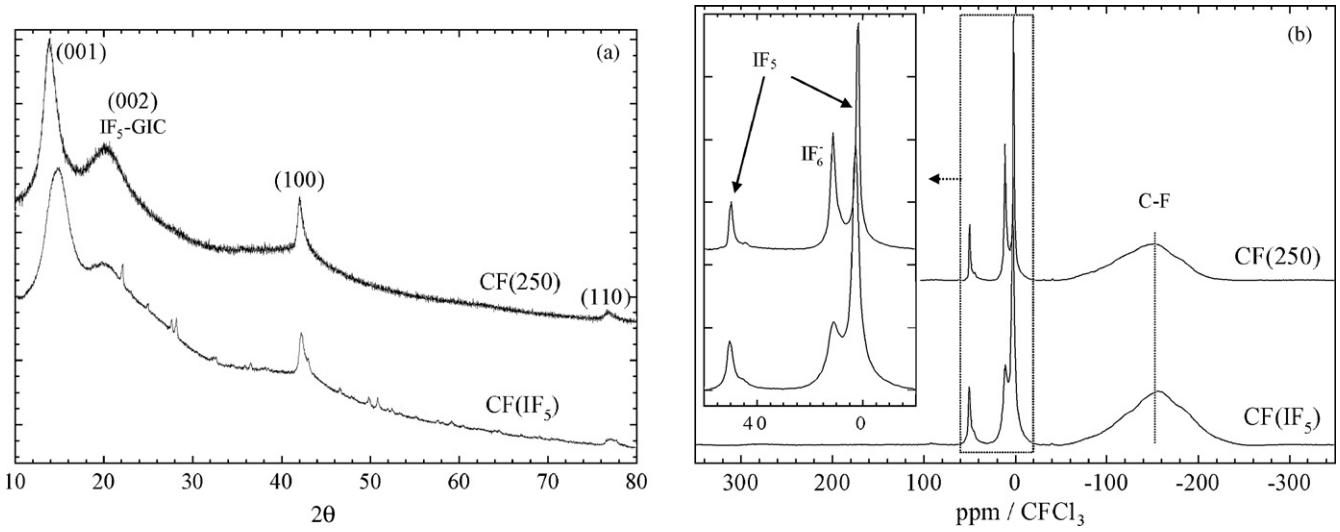

Fig. 2. (a) X-ray diffraction patterns of $CF(IF_5)$ and CF(250). (b) ^{19}F MAS spectra, at 12 kHz, of $CF(IF_5)$ and CF(250).

−20/60 ppm zone. The decrease of the NMR lines area, evidenced by their narrowing is characteristic of a decrease of the iodine content. Moreover, a conversion of IF_5 into IF_6^- simultaneously occurs [23]. Over the −200/−100 ppm range, the spectra exhibit a broad band at −160 ppm, attributed to iono-covalent C–F bonds [21–23]. The corresponding line does not seem to be affected by the re-fluorination treatment, but owing to its large width a shift is difficult to detect. However, an infra-red study had previously shown [21] that the C–F bond covalency is slightly increased in such conditions.

3.2. Electrochemical properties

3.2.1. Electrochemical reaction

The galvanostatic discharge curves of $CF(IF_5)$, in the different electrolytes (0.5 or 1 M $Mg(ClO_4)_2$ in ACN, DMSO, PC or THF), are shown Fig. 3. These electrolytes were chosen because they have been commonly used in magnesium batteries. The plateau observed are characteristic of this family of materials [14,24,25].

In order to investigate the electrochemical reaction, ^{19}F NMR was carried out on two discharged electrodes (full discharge and ≈50%) in ACN based electrolyte. Fig. 4 displays the MAS spectrum of the reduced electrodes, the electrode binder (PVDF), the crystalline MgF_2 and the starting $CF(IF_5)$ material.

The lines of the binder, at −92 and −115 ppm, appear on the spectrum of the discharge electrode composite; their line width are broadened in comparison with the raw PVDF. The binder is not totally inert and interacts with the electrolyte and/or with the active material.

The discharge mechanisms of Mg/CF_x and Li/CF_x cells are close concerning several points:

(i) After the reduction, the narrow lines of iodine species (≈2 and 50 ppm for IF_5 species and ≈11 ppm for IF_6^- ions) drastically decrease; this indicates that iodine fluoride species are removed from the host material, in accordance with the colour change of the electrolyte relative to the reduction of the catalyst residues into iodine. Nevertheless, this resonance at +20 ppm is still present and could be related to solvated fluorides (such as IF_6^- or reduced fluorides) removed from the host matrix and transferred into the electrolyte. This contaminated electrolyte could wet the surface of the sample. In the case of Li/CF_x cell, the content of IF_6^- vary as a function of the sample conditioning but the change of the line profile on NMR spectra shows their partial or total removal [26].

(ii) The broad line entered at −160 ppm, which is typical of C–F bonds in the rigid matrix of fluorinated graphite compounds is also significantly lowered on the spectrum of the 50% reduced sample. Through the breaking of the C–F bonds, the host matrix is partly electroreduced. For the fully reduced sample the broad band has almost disappear; indicating a quasi-total reduction of the C–F groups.

(iii) After complete reduction, an additional narrow line is present at −128 ppm. This latter is assigned to CF_2 groups [27], this line appears only as a shoulder of the main C–F group line (−160 ppm) for the 50% discharged sample. Some CF_2 groups are present into the raw CF_x sample but owing to the broad line of the C–F group and the weak CF_2/CF ratio, they are not visible on the ^{19}F MAS spectra. These groups are known to be electrochemically inactive (because they require too much energy to be reduced); after reduction they are still present in opposite to CF groups.

(iv) In the case of Li/CF_x cell, LiF is formed during the discharge. MgF_2 is then expected as product of the electrochemical process for Mg/CF_x cell. The line at −198 ppm and the corresponding sidebands are similar to the spectrum of MgF_2 [28,29], which is added for comparison in Fig. 4. This unambiguously confirms the formation of this fluoride during the discharge. The line of the electrochemically formed MgF_2 is broader than for the crystallized reference sample; this could result from a more disorganized state for the discharge product. As a matter of fact, X-ray diffraction patterns hardly show MgF_2 peaks (Fig. 5). Most intense reflections of the

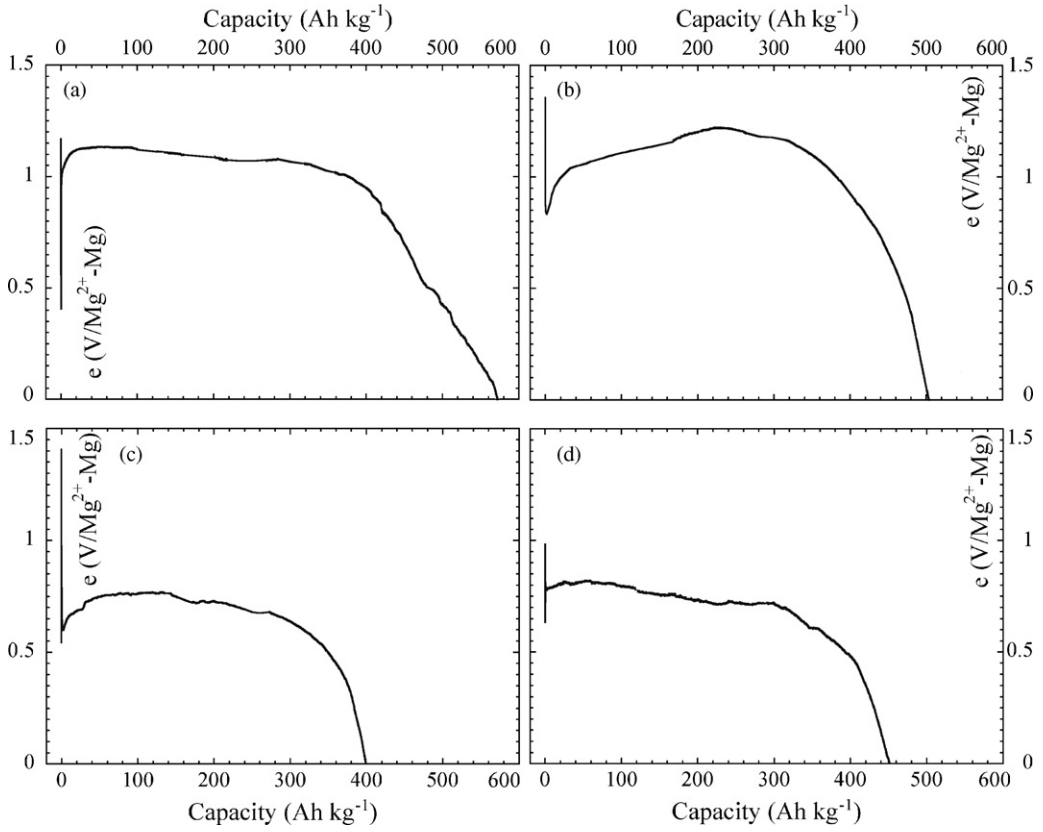

Fig. 3. Galvanostatic discharges curves (10 A kg^{-1}, RT) of CF(IF_5) for different electrolytes: (a) 1 M $Mg(ClO_4)_2$/ACN, (b) 0.5 M $Mg(ClO_4)_2$/DMSO, (c) 1 M $Mg(ClO_4)_2$/PC and (d) 1 M $Mg(ClO_4)_2$/THF (+3.33 M H_2O/THF).

crystalline sellaite MgF_2 are attempted at $d_{1\,1\,0} = 0.327$ nm ($2\theta = 27.25°$), $d_{1\,1\,1} = 0.223$ nm (40.42°), $d_{2\,1\,0} = 0.207$ nm (43.69°), $d_{2\,1\,1} = 0.171$ nm (53.55°), $d_{2\,2\,0} = 0.163$ nm (56.40°) and $d_{3\,0\,1} = 0.138$ nm (68.14°). Such peaks have been detected only for the X-ray diffraction patterns of the 100% discharged electrode and annealed at 250 °C under air atmosphere during 8 h before analysis. The annealing procedure leads to an enhancement of the MgF_2 crystallinity. So, the presence of amorphous state of MgF_2 in the discharged electrode material is confirmed by XRD. Moreover, concerning the fluorocarbon matrix, the quasi-disappearance of the peak located at 14°, which is assigned to (0 0 1) reflection of graphite fluoride matrix, argues for the CF_x reduction. It must be noted that the additional peaks are assigned to electrolyte residues ($Mg(ClO_4)_2$, $6H_2O$), catalyst traces used during low temperature graphite fluoride synthesis (IF_5, IF_6^-) and graphite used as a conductive additive during electrode preparation.

Thanks to X-ray diffraction and ^{19}F NMR, the latter allows to specifically investigating the fluorinated compounds i.e. the fluorocarbon host matrix and MgF_2 but also the PVDF binder, an electrochemical reaction can be proposed for the discharge of the Mg/CF_x cell:

$$CF_x + \frac{x}{2}Mg^{2+} + xe^- \rightarrow C + \frac{x}{2}MgF_2 \quad (1)$$

3.2.2. *Effects of the electrolyte composition and of the re-fluorination treatment*

As observed in Fig. 3, the average discharge potentials $E_{1/2}$, measured at half of the maximal capacity, are 1.08, 1.20, 0.73 and 0.72 V for the ACN, DMSO, PC and THF based electrolyte, respectively. Data on the average discharge potential ($E_{1/2}$), specific capacity (C), specific energy (E_s) and specific power (P_s) are detailed in Table 1. The highest $E_{1/2}$ value is obtained in DMSO.

The discrepancy observed regarding the different solvents could be explained by a more or less easy diffusion and/or dissolution of Mg^{2+} from the electrode to the electrolytes. Indeed, the formation of a passivating layer at the surface of a magnesium anode has often been invoked in earlier works dedicated to magnesium batteries [30–34]. The latter is currently recognised as highly impermeable to Mg^{2+} ions, the mobility of the Mg^{2+} ions in the passivating films being extremely low [30–34]. Magnesium dissolution, can then only occur at a high overpotential, via a mechanism involving rupture of the film, as suggested in Refs. [31–33]. The dissolution of Mg^{2+} seems then facilitated in the order THF = PC < ACN < DMSO.

One may also infer that the corresponding potential decrease is different for each electrolyte because Mg^{2+} solvation depends on the nature of the solvent. The role played by solvation, may then lie in the respective sizes of the solvation spheres of the cation from one medium to another one. Thus, insertion of Mg^{2+} into the materials is all the more hindered and the resulting poten-

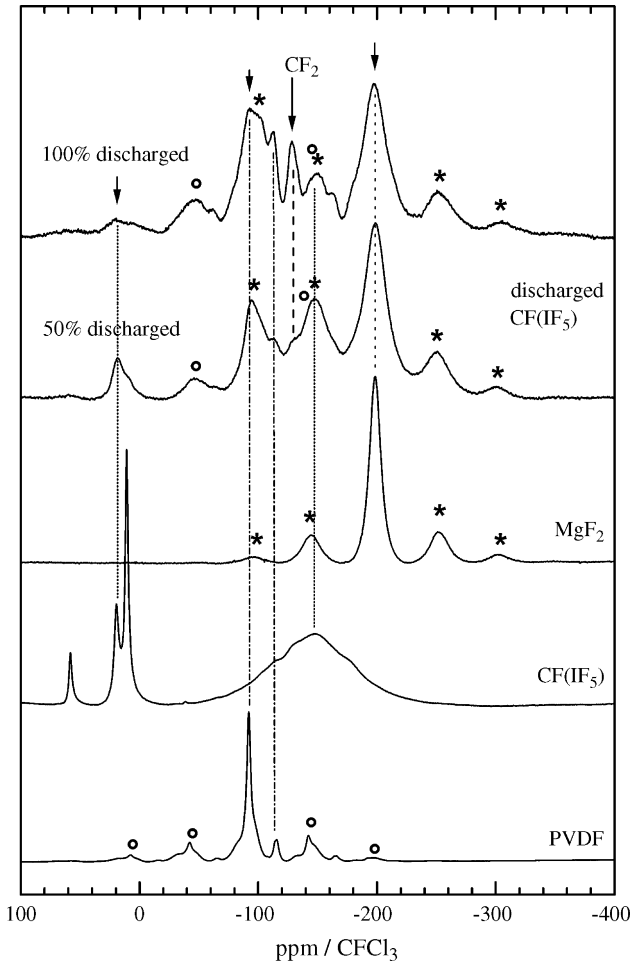

Fig. 4. ^{19}F NMR spectra, at 14 kHz, of the discharged electrode $CF(IF_5)$ (fully and 50% discharged) and the raw graphite fluoride. The spectra of the reference compounds, crystalline MgF_2 and PVDF binder are added for comparison. '*' and '○' mark the spinning sidebands of MgF_2 and PVDF, respectively.

tial drop all the more notable that the solvation of Mg^{2+} species is strong. In addition, the potential drop could also result from a partial desolvation occurring at the surface of the host material before intercalation, as suggested in Ref. [30].

The theoretical capacity is related to the reduction scheme (1). The transformation of CF_x into carbon and MgF_2 is responsible for the irreversibility of the system. The theoretical maximum capacity is then 756 Ah kg^{-1} for $CF(IF_5)$. However, the highest experimental capacity obtained is 572 Ah kg^{-1}. The presence of residual iodine fluorides can hinder magnesium penetration

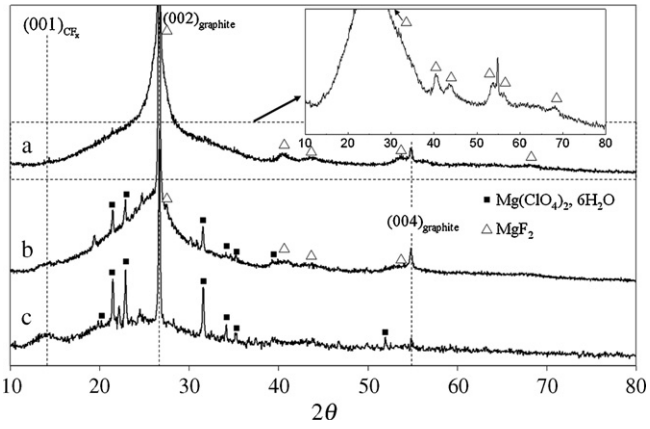

Fig. 5. X-ray diffraction patterns of the discharged electrode $CF(IF_5)$: fully (a) and (b) and 50% discharged (c). Before analysis sample (a) have been heat-treated during 8 h at 250 °C under air atmosphere.

into the host lattice and therefore accessibility to the C–F sites, leading to a reduced experimental capacity.

The specific energy density E_s and power density P_s are two important parameters characterising a battery, that can be obtained from the discharge curves (see Table 1). As for the capacity and average discharge potential, the most interesting values of the energy and power densities are also obtained in ACN and DMSO electrolytes. For these two solvents, E_s and P_s are of the same order: E_s = 600–620 W kg^{-1} and P_s = 10–12 Wh kg^{-1}. For the two other electrolytes, E_s and P_s are divided by a factor close to 2.

A subsequent heat-treatment under fluorine can be used for strengthening the C–F bond [21,22]. From an electrochemical view point, this results in a decrease of the average discharge potential: the higher the covalency, the lower $E_{1/2}$, since this potential is related to the Gibbs free energy of dissociation of the C–F bond, that occurs in the course of reaction (1). Thus, a preliminary test was realized in order to verify to which extent this behaviour is followed upon association with a magnesium anode. For 1 M $Mg(ClO_4)_2$/PC, $E_{1/2}$ evolves from 0.73 to 0.68 V after the annealing procedure (Fig. 6). In parallel, the capacity increases from 400 to 429 Ah kg^{-1}. The re-fluorination treatment yields a higher F/C ratio and therefore a slightly improved capacity. In addition, the weaker content of residual iodine fluorides species, which likely hinder cationic diffusion into the cathodic material, is also an argument in favour of the capacity increase.

Table 1
Galvanostatic characteristics of Mg/$CF(IF_5)$ and Mg/CF(250) batteries obtained at room temperature for different electrolytes

Sample	Electrolytic solvent	$E_{1/2}$ (V)	Capacity (Ah kg^{-1})	Specific energy (Wh kg^{-1})	Specific power (W kg^{-1})
$CF(IF_5)$	ACN	1.08	572	618	10.8
	DMSO	1.20	503	604	12.0
	PC	0.73	400	292	7.3
	THF	0.72	451	325	7.2
CF(250)	PC	0.68	429	292	6.8

$E_s = C^*E_{1/2}$ (Wh kg^{-1}) and $P_s = d^*E_{1/2}$ (W kg^{-1}). C and d are the discharge capacity (Ah kg^{-1}) and the current density (A kg^{-1}), respectively. d = 10 A kg^{-1} for all tests.

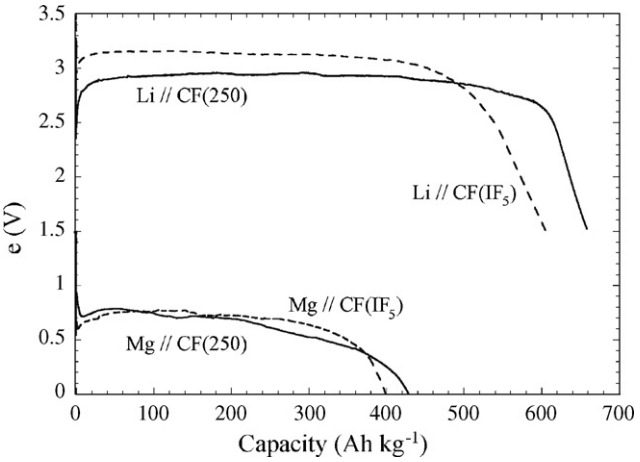

Fig. 6. Galvanostatic discharge curves (10 A kg^{-1}, RT) of $CF(IF_5)$ and CF(250) as lithium cathodes (1 M $LiClO_4$/PC) and of $CF(IF_5)$ and CF(250) as magnesium cathode (1 M $Mg(ClO_4)_2$/PC).

3.2.3. Comparison with lithium anodes

Graphite fluorides prepared at high temperature have been used as cathodes in commercial lithium batteries over many years. Therefore, a compound similar to the present $CF(IF_5)$ sample had been previously studied as a new component likely to enter into such a system [24,25]. It is then interesting to compare the results obtained from lithium and magnesium. The galvanostatic discharge curve of $CF(IF_5)$ used in a lithium battery with 1 M $LiClO_4$/PC as electrolyte is shown in Fig. 6. The theoretical optimal capacities are identical for both lithium and magnesium (756 Ah kg^{-1}). This value is however never reached, the capacity obtained upon magnesium accommodation being the lowest. This phenomenon has often been observed in other studies [6,30,35]. The poorer efficiency in the case of magnesium cells may be explained by a more difficult diffusion of Mg^{2+} into the material in comparison with Li^+. The hindering due to IF_z species may more strongly reduce the accessibility of magnesium to reactive sites.

The average discharge potential is 1.9 V lower for magnesium in regard to lithium, whereas the theoretical potential drop expected from the difference in the Gibbs free energy of formation of LiF and MgF_2, when put in the Nernst equation ($\Delta E_{1/2} \approx \Delta E^\circ = E^\circ_{Li} - E^\circ_{Mg} = -1/F(\Delta G^\circ_{LiF} - 1/2\,\Delta G^\circ_{MgF_2})$), would be 0.6 V. Such a difference is a good indication that a high overpotential takes place, owing to the existence of a passivating layer on the magnesium electrode.

In the case of magnesium batteries, we have presently shown that the heat-treatment performed on the fluorinated cathodic material leads to a modification of the electrochemical properties: $E_{1/2}$ diminution (−0.05 V) and capacity increase (7%). A similar behaviour is observed for lithium, i.e. an $E_{1/2}$ diminution by −0.16 V accompanied by a simultaneous improvement of the capacity by 10% (Fig. 6). Both the energy and power values remain unchanged after the fluorination post-treatment for the two kinds of batteries. Nevertheless, in magnesium-based cells the energy and power densities are reduced by a factor of at least 3 in comparison with lithium systems.

4. Conclusion

In this study, the insertion of Mg^{2+} ions into graphite fluorides has been investigated for the first time. Among the four solvents used, ACN and DMSO based electrolytes give the highest capacity (572 Ah kg^{-1} in the case of ACN) and average discharge potential (1.20 V, for DMSO), yielding consequently the best performances regarding specific energy and power: ≈610–620 and ≈10–12 W kg^{-1}, respectively.

The Mg/graphite fluoride system provides reduced overall electrochemical performances in comparison with an equivalent lithium system. Nevertheless, this preliminary approach shows that graphite fluorides could be an interesting alternative for the development of novel magnesium battery technologies. We suggest that serious improvements may be obtained at the cathode level via re-fluorination treatments, whose effects on the electrochemical properties require complementary studies. In parallel, research on the elaboration of an electrolyte which does not quench the electrochemical performances must be performed. The use of solutions of Grignard reagent or solid electrolytes have been evoked. More investigation is needed on both the cathode material and global process before applications can emerge.

References

[1] M. Winter, J.O. Besenhard, M.E. Spahr, P. Novak, Adv. Mater. 10 (1998) 725–763.
[2] S. Whittingham, Chem. Rev. 104 (2004) 4271–4302.
[3] D. Aurbach, I. Weissman, Y. Gofer, E. Levi, Chem. Rec. 3 (2003) 61–73.
[4] L. Yu, X. Zhang, J. Colloid Interf. Sci. 278 (2004) 160–165.
[5] L. Jiao, H. Yuan, Y. Wang, J. Cao, Y. Wang, Electrochem. Commun. 7 (2005) 431–436.
[6] M.E. Spahr, P. Novak, O. Haas, R. Nesper, J. Power Sources 54 (1995) 346–351.
[7] L. Sanchez, J.P. Pereira-Ramos, J. Mater. Chem. 7 (1997) 471–473.
[8] T.D. Gregory, R.J. Hoffman, R.C. Winterton, J. Electrochem. Soc. 137 (1990) 775–780.
[9] W. Yuan, J.R. Gunter, Solid State Ionics 76 (1995) 253–258.
[10] D. Aurbach, Z. Lu, A. Schechter, Y. Gofer, H. Gizbar, R. Turgeman, Y. Cohen, M. Moshkovich, E. Levi, Nature 407 (2000) 724–727.
[11] R. Yazami, in: T. Nakajima (Ed.), Fluorine–Carbon and Fluoride–Carbon Materials: Chemistry, Physics, and Applications, Marcel Dekker, New York, 1995, pp. 251–281.
[12] T. Nakajima, N. Watanabe, in: T. Nakajima (Ed.), Graphite Fluorides and Carbon–Fluorine Compounds, CRC Press, Boca Raton, FL, 1991, pp. 84–89.
[13] N. Watanabe, Solid State Ionics 1 (1980) 87–110.
[14] R. Yazami, A. Hamwi, Solid State Ionics 28–30 (1988) 1756–1761.
[15] R. Hagiwara, W. Lerner, N. Bartlett, T. Nakajima, J. Electrochem. Soc. 135 (1988) 2393–2394.
[16] T. Nakajima, M. Koh, V. Gupta, B. Zemva, K. Lutar, Electrochim. Acta 45 (2000) 1655–1661.
[17] M.J. Root, R. Dumas, R. Yazami, A. Hamwi, J. Electrochem. Soc. 148 (2001) 339–345.
[18] G. Levitin, C. Yarnitzky, S. Licht, Electrochem. Solid State Lett. 5 (2002) 160–163.
[19] A. Hamwi, M. Daoud, J.C. Cousseins, Synth. Metals 26 (1988) 89–98.
[20] A. Hamwi, R. Yazami, Patent WO90/07798 (1990).
[21] K. Guérin, J.P. Pinheiro, M. Dubois, Z. Fawal, F. Masin, R. Yazami, A. Hamwi, Chem. Mater. 16 (2004) 1786–1792.
[22] M. Dubois, K. Guérin, J.P. Pinheiro, Z. Fawal, F. Masin, A. Hamwi, Carbon 42 (2004) 1931–1940.

[23] J. Giraudet, M. Dubois, K. Guérin, J.P. Pinheiro, A. Hamwi, W.E.E. Stone, P. Pirotte, F. Masin, J. Solid State Chem. 178 (2005) 1262–1268.
[24] K. Guérin, R. Yazami, A. Hamwi, Electrochem. Solid State Lett. 7 (2004) 159–162.
[25] J. Giraudet, C. Delabarre, K. Guérin, M. Dubois, F. Masin, A. Hamwi, J. Power Sources 158 (2006) 1365–1372.
[26] K. Guérin, M. Dubois, A. Hamwi, J. Phys. Chem. Solids 67 (5–6) (2006) 1173–1177.
[27] T.R. Krawietz, J.F. Haw, Chem. Commun. 19 (1998) 2151–2152.
[28] A.T. Kreinbrink, C.D. Sazavsky, J.W. Pyrz, D.G.A. Nelson, R.S. Honkonen, J. Magn. Reson. 88 (1990) 267–276.
[29] J. Krishna Murthy, U. Groβ, S. Rüdiger, E. Ünveren, E. Kemnitz, J. Fluorine Chem. 125 (2004) 937–949.
[30] P. Novak, R. Imhof, O. Haas, Electrochim. Acta 45 (1999) 351–367.
[31] D. Aurbach, R. Turgeman, O. Chusid, Y. Gofer, Electrochem. Commun. 3 (2001) 252–261.
[32] D. Aurbach, Y. Gofer, Z. Lu, A. Schechter, O. Chusid, H. Gizbar, Y. Cohen, V. Ashkenazi, M. Moshkovich, R. Turgeman, E. Levi, J. Power Sources 97/98 (2001) 28–32.
[33] Z. Lu, A. Schechter, M. Moshkovich, D. Aurbach, J. Electroanal. Chem. 466 (1999) 203–217.
[34] J.O. Besenhard, M. Winter, Chem. Phys. Chem. 3 (2002) 155–159.
[35] P. Novak, W. Scheifele, O. Haas, J. Power Sources 54 (1995) 479–482.